



Local Wave Energy Dissipation and Morphological Beach Characteristics along a Northernmost Segment of the Polish Coast

Grzegorz Różyński

Institute of Hydro-Engineering, Polish Academy of Sciences, ul. Kościarska 7, 80-953 Gdańsk, Poland
e-mail: grzegorz@ibwpan.gda.pl

(Received September 05, 2018; revised November 22, 2018)

Abstract

This paper analyses cross-shore bathymetric profiles between Władysławowo (km 125 of the Polish coastal chainage) and Lake Sarbsko (km 174) done in 2005 and 2011. Spaced every 500 m, they cover beach topography from dune/cliff crests to a seabed depth of about 15 m. They were decomposed by signal processing techniques to extract the monotonic component of beach topography and to perform a straightforward assessment of wave energy dissipation rates. Three characteristic dissipation patterns were identified: one associated with large nearshore bars and 2–3 zones of wave breaking; a second, to which the equilibrium beach profile concept can be applied; and a third, characterized by mixed behaviour. An attempt was then made to interpret these types of wave energy dissipation in terms of local coastal morphological features and the underlying sedimentary characteristics.

Key words: coastal morphology; wave energy dissipation; equilibrium profiles; data-driven modelling; signal processing

1. Introduction

The idea of ‘the beach equilibrium profile’ was first used by Bruun (1954), who assumed that cross-shore beach topography is basically a function of wave energy E supplied to the shore at a shallow-water group wave velocity c_g and then concluded that nearshore seabed configurations are best described by monotonic power functions:

$$h(x) = A \cdot x^n. \quad (1)$$

In Eq. (1), h is the seabed depth at the offshore distance x from the shoreline, and the parameters A and n are empirical quantities.

The theoretical background of the equilibrium beach configuration in constant hydrodynamic regimes was developed by Dean (1976), who postulated the invariance of wave energy dissipation E_r across the entire surf zone. Other assumptions included

cross-shore sediment homogeneity ($D_{50} = \text{const}$), monochromatic waves, linear wave theory and a constant wave breaking index $\gamma = H/h = \text{const}$. As a result, the wave energy dissipation rate was expressed by the equation in which the only morphological parameter is the depth of the seabed h and its derivative:

$$E_r = \frac{5}{16} \rho g^{3/2} \gamma^2 h^{1/2} \frac{dh}{dx}. \quad (2)$$

Assuming the invariance of E_r , the well-known monotonic power function emerged:

$$h(x) = A \cdot x^{2/3}. \quad (3)$$

The coefficient A has a dimension of $[\text{m}^{1/3}]$ and is directly related to E_r :

$$A = \left(\frac{24E_r}{5\rho g^{3/2} \gamma^2} \right)^{2/3}. \quad (4)$$

In Eq. (4), $g = 9.81 \text{ m/s}^2$ is the acceleration of gravity, $\rho = 1000 \text{ kg/m}^3$ is the specific gravity of water, and $\gamma = 0.78$ is the wave breaking index. The constant wave energy dissipation is known as the saturated wave breaking regime. It reflects the situation in which invariant hydrodynamic conditions tend to produce an equilibrium seabed configuration.

The relationships between the coefficient A and physical parameters of beach sediment were first investigated by Moore (1982). Next, Dean (1987) related this coefficient to the sediment fall velocity w_s with the formula $A = 0.067(w_s)^{0.44}$. A similar contribution by Kriebel et al (1991) yielded another straightforward relationship:

$$A \approx 2.25 \left(\frac{W_s}{g} \right)^{1/3}. \quad (5)$$

A temporal dependence of beach equilibrium profiles was investigated by Pruszk (1993), who introduced a time-varying coefficient A as a sum of components oscillating over time:

$$A(t) = \bar{A} + A_1 + A_2 + A'. \quad (6)$$

In this expression, \bar{A} is the time-invariant component expressed through e.g. Eq. (5), A_1 represents long-term variations due to the migration of large bed forms or changes in sediment supply, driven by the long-term variability of the hydrodynamic background, A_2 accounts for seasonal variations, and A' corresponds to individual events, such as storms. The periodic behaviour of the beach equilibrium profile can be presented as

$$A(t) = \sum_{k=1}^2 a_k \cos \left(2\pi \frac{t}{T_k} + \theta_k \right) + A'. \quad (7)$$

The periods T_k correspond to long ($k = 1$) and medium (seasonal) time scales ($k = 2$); the period T_1 was found to be approximately 27 years for the Polish coast.

A different contribution was proposed by Inman et al (1993), who assumed a model in which the offshore part of the profile was treated independently of the inner bar-berm portion, and both were matched at the breakpoint bar. Such division was justified by different forcing modes on either side of the breakpoint. Both portions were fitted well by Eq. (1), with $n \approx 0.4$ being nearly the same for the bar-berm portion and the outer portion, irrespectively of seasonal changes. In this way, changes in seasonal equilibriums could be manifested by self-similar displacements of the bar-berm and outer curves, driven by seasonal surf zone variations.

Bodge (1992) addressed two major drawbacks of previous formulations, namely the physically unrealistic offshore-infinite range of beach equilibrium profiles and the infinite slope at the shoreline. An exponential curve was therefore proposed, asymptotically converging to the closure depth to describe the beach equilibrium profiles. This concept was further improved by Komar and McDougal (1994), who replaced the closure depth with a ratio of the shoreline beach slope S_0 to the empirical parameter k [m^{-1}] accounting for profile concavity:

$$h(x) = \frac{S_0}{k(1 - e^{-kx})}. \quad (8)$$

This model predicts asymptotic convergence to a depth of S_0/k meters for the shoreline beach slope S_0 , which can be determined as a function of sediment grain size and wave parameters or evaluated directly from profile measurements. Then, only the concavity parameter k should be least-square fitted to profile measurements.

Several alternative approaches have been proposed to tackle shoreline singularity. Larson and Kraus (1989) suggested a form that superimposed a planar shallow water component on an offshore Dean form. Özkan-Haller and Brundidge (2007) introduced a further modification to confine the influence of the planar component to shallow water. Perhaps the most advanced model was presented by Holman et al (2014), who developed an equilibrium beach profile concept capable of accounting for a) a finite shoreline slope, b) a concave-up form in wave-dominated shallow waters and c) an asymptotic planar slope in the far field:

$$h(x) = \alpha(1 - e^{-kx}) + \beta x. \quad (9)$$

This model requires three parameters: a) the far-field slope β can be obtained directly from available bathymetric charts, b) the shoreline slope can also be easily determined using the expression $d(h=0)/d(x=0) = S_0 \Rightarrow S_0 = \alpha k + \beta$, and c) the depth h should be known at some location x' , which can be anywhere in the profile, but should be representative of the background, average profile depth, so it should best be a point seaward of the active bar zone. This last parameter is therefore subjective to some extent, but is necessary to determine the second equation relating α and k : $h(x') = \alpha(1 - e^{-kx'}) + \beta x'$.

The conceptual simplicity and modelling robustness of beach equilibrium profiles resulted in their wide acceptance. In particular, equilibrium profiles are used extensively in beach-fill design studies and projects, see e.g. CEM (2008) Part III-3, or CEM (2008) Part V-4. The major underlying reason is that the complicated and non-linear phenomena of wave energy dissipation are often intractable by most physical models, particularly in systems with multiple bars (Różyński 2003). It can be briefly explained as follows:

- 1) When waves are mild, the surf zone is narrow, and they break only over the innermost bar.
- 2) Higher waves begin to break over the 2nd bar; the surf zone now includes two bars, and the breakers can include a spilling or a plunging mode or both.
- 3) During heavy storms, the outer bars contribute to wave energy dissipation as well – the surf zone now includes 4 bars or more and is several hundred meters wide. Various combinations of spilling and plunging modes are then possible, resulting in very complicated longshore and cross-shore sediment transport patterns.
- 4) Variations of wave set-up and wind-driven storm surges (in a range of 1 meter) further modify breaking regimes during the build-up, peak and recession of storms.

The insufficient robustness of physical models to successfully deal with complex surf zone morphodynamic processes necessitates other tools that can provide some insight into the evolution of complicated coastal bathymetries. One such solution was proposed by Różyński and Lin (2015), who developed the concept of empirical equilibrium profiles. These profiles originate from actual bathymetric measurements and are derived by extraction of their monotonic component, which usually contains more than 90% of overall profile variability. Empirical equilibrium profiles relax the main assumption of theoretical Dean-type equilibrium profiles, namely the constant wave energy dissipation rate in the entire surf zone. In addition, if an empirical equilibrium profile closely resembles the shape of a Dean function, it demonstrates that saturated wave breaking regimes can be encountered in reality, at least along some portion of the surf zone, usually closer to the shoreline.

Empirical equilibrium profiles can be extracted from measured cross-shore seabed configurations by signal processing methods, such as Empirical Mode Decomposition (EMD), see (Różyński and Lin 2015), or Singular Spectrum Analysis (SSA), see (Różyński et al 2001). The only constraint is the monotonicity of empirical equilibrium profiles. It is needed to secure the applicability of Eq. (2), in which changes in wave energy dissipation intensity are governed primarily by the 1st derivative of the empirical equilibrium profile and secondarily by the square root of that profile. The positive sign of the derivative is needed to sustain wave energy dissipation. This equation is very useful because the resulting rates of energy dissipation are continuous, smooth and can be easily computed. Moreover, departures from actual dissipation rates are not very significant, because empirical equilibrium profiles usually contain more than 90% of profile variability.

The goal of the paper was to relate the identified wave energy dissipation patterns to local, man-made or natural, coastal morphological features along a fairly long and diverse coastal segment in Poland between the western breakwater of the Władysławowo harbour (km 125 of the national coastal chainage) and a beach east of Lake Sarbsko (km 174), see (Różyński and Szmytkiewicz 2018). Wave energy dissipation patterns were identified using the empirical equilibrium profile concept for two sets of geodetically fixed bathymetric profiles measured in 2005 and 2011 for monitoring purposes. Special attention was given to evaluation of the resemblance between empirical and theoretical Dean profiles in areas where saturated wave breaking regimes are encountered.

2. Data and Methodology

Fig. 1 presents the Polish coast and shows both ends of the national coastal chainage at km 0 (border with Russia) and km 428 (border with Germany). It also presents the limits of the study area at km 125 and 174. The profile lines, surveyed in 2005 and 2011 in the study area, are geodetically fixed and spaced every 500 m, providing a data base with almost 100 profiles sampled twice. Their cross-shore range covers the area from the dune/cliff crest to a depth of 15 m or more; it normally measures more than 2,000 m.



Fig. 1. General map of Polish coastline, after (Różyński and Szmytkiewicz 2018)

A significant onshore and offshore extension of the profile lines offers a perfect opportunity for the exact extraction of their key modes of variability, as the extensive coverage of beach and seabed topography reduces the so-called end effects that can distort the modes of variability near both profile extremities. One of data-driven techniques used for the extraction of the modes of variability, well tested in coastal applications, is the Singular Spectrum Analysis (SSA). Briefly, it consists in evaluation of the covariance structure of each profile and the computation of the associated modes of variability, known as the reconstructed components. If the number of points in a profile is n , then the number of modes of variability should not exceed $1/3n$ to

eliminate inaccurate estimation of higher modes. The modes are ranked according to the portion of total signal (profile) variance each of them contains, starting from the one with the largest contribution. Reconstructed components are additive and can be summed, starting from the most significant one to the mode whose inclusion destroys the monotonic feature of the empirical equilibrium line. The profiles studied usually contained 210–220 elements, so the maximum number of modes was set at $m = 70$. However, the number of modes that contributed to empirical equilibrium profiles was found to be much less, usually no more than 5.

3. Results

Fig. 2 shows fractions of profile variances explained by empirical equilibrium profiles for the survey of 2005. They were calculated for $N = 50$ profiles, so the span between the profiles was 1 km. The average variance fraction explained by empirical equilibrium profiles was 92%, the related median 94.9%, the minimum 66.5%, and the maximum 99.3%. On the basis of Fig. 2, we decided to scrutinize in detail 6 representative profiles whose explained variance is near the average value (km 130, 149 and 156) or significantly departs from that value (km 125, 139 and 161). These 6 profiles are marked in Fig. 2.

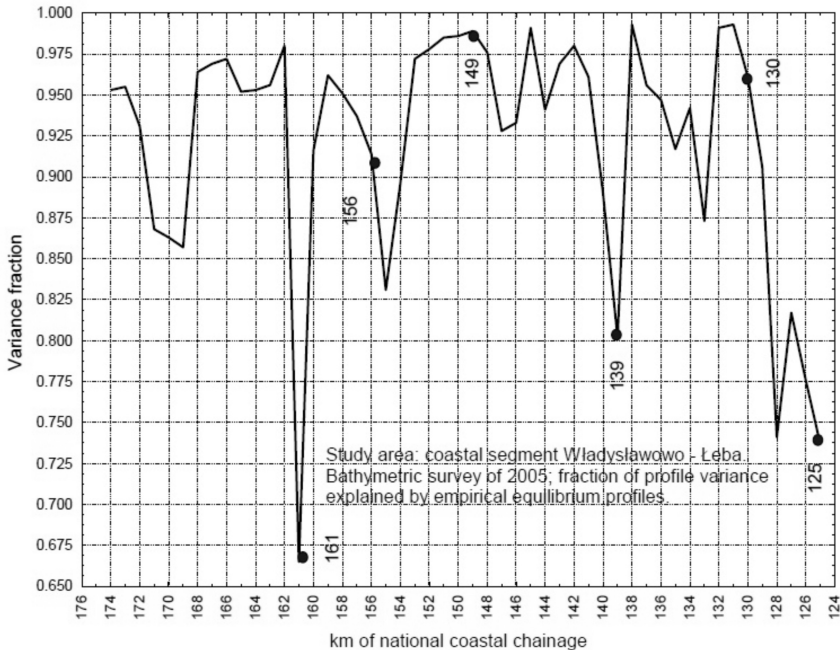


Fig. 2. Fraction of profile variance explained by empirical equilibrium profiles, after (Różyński and Szmytkiewicz 2018)

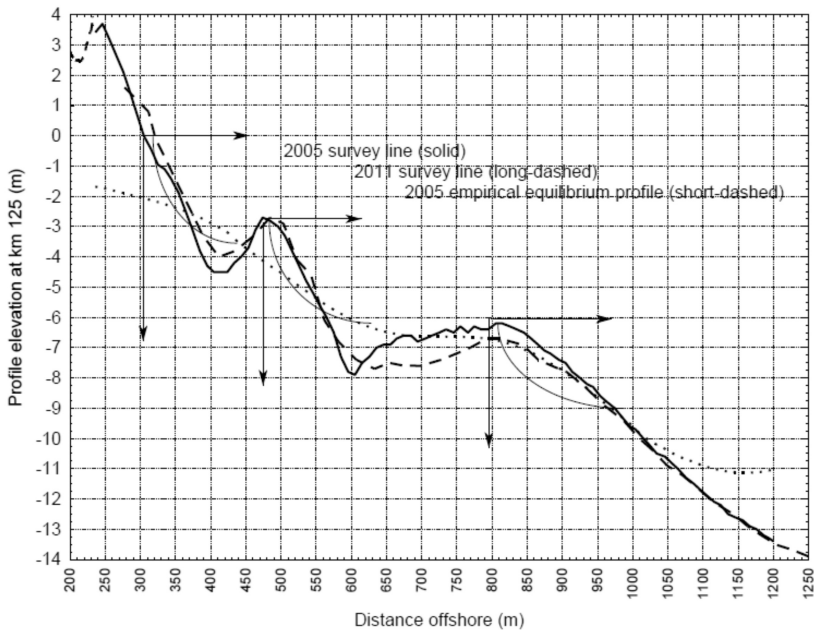


Fig. 3. Empirical equilibrium profile at km 125, after (Różyński and Szmytkiewicz 2018)

Fig. 3 presents the analysis for km 125. The morphology of both surveys is very similar, dominated by two very large nearshore bars. Owing to the resemblance between them, SSA decomposition was done for the 2005 seabed configuration only. The empirical equilibrium profile contains only one mode of variability, which departs significantly from the measured seabed configuration (cf. Fig. 2) and contains only 73.7% of the original profile variability. However, the addition of another mode of variability destroys the monotonicity of empirical equilibrium profile instantly. This result demonstrates that the concept of one surf zone with wave breaking processes distributed continuously across its entire cross-shore range cannot be accepted at this location, because the prominence of bars results in a system with intensive wave breaking processes along the offshore bar slopes and zones without dissipation of wave energy inside the troughs. It was schematized by plotting three systems of coordinates, fixed at the shoreline and bar crests, for which separate Dean curves, representing disjoint sub-zones of wave energy dissipation, could be postulated. No saturated wave energy dissipation can be expected for this location, and the monotonic profile cannot describe wave energy dissipation with sufficient precision. More generally, large bars indicate local sediment saturation, as km 125 is situated on the updrift side just west of the breakwater of the Władysławowo harbour, constructed in the late 1930s. The abundance of sediment results from the initial blockage of littoral drift by that breakwater, running perpendicularly to the natural coastline. Thus, km 125 represents local conditions drastically altered by deep anthropogenic intervention and demonstrates that

the proposed methodology correctly identified that situation. Neither of these seabed configurations shows noteworthy variations over the 6 years, so it can be implied that this system has reached stability and currently remains in long-term equilibrium. The equilibrium conditions coincide with the naturally re-established by-passing of sediment that generally runs from west to east (Szymkiewicz et al 1998). Significant initial shoreline advance west of the harbour breakwater, cf. (Szymkiewicz et al 1998), and the very large bars existing currently under conditions of west-to-east littoral drift are therefore direct consequences of the harbour construction in the 1930s. A study on local sediment composition and cross-shore distribution at km 125 is recommended to ascertain the history of sediment deposition in that area after the harbour construction. Its results should then be compared with the parameters of native sediment; any differences between the native and deposited sediment parameters will indicate the effects of the harbour construction on local hydro- and morphodynamics and illustrate the process of re-establishment of natural sediment migration.

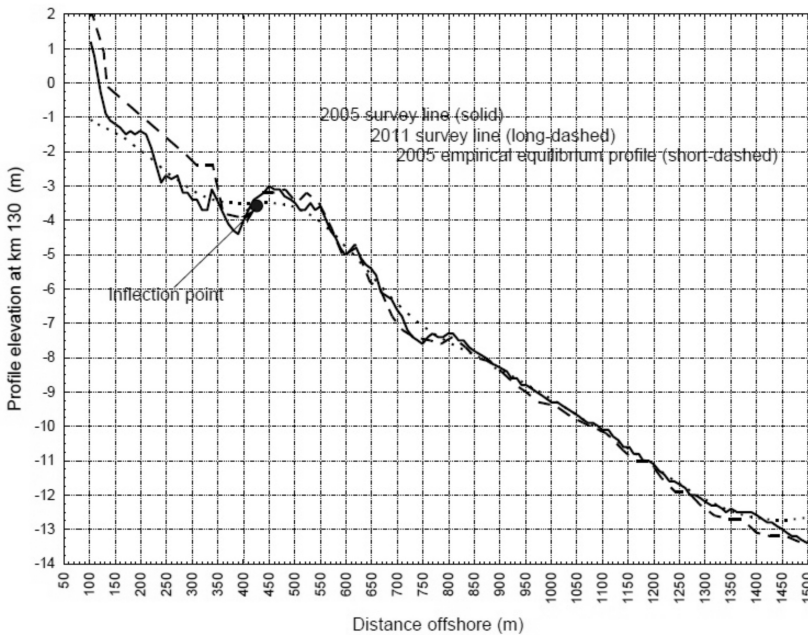


Fig. 4. Empirical equilibrium profile at km 130, after (Różyński and Szymkiewicz 2018)

Fig. 4 represents the analysis done for km 130 near Chłapowo, at the eastern end of a soft cliff of post-glacial origin, running from Chłapowo to Jastrzębia Góra. Both surveys show one dominant bar with a crest situated about 400 m from the shoreline, which is preceded by a distinct trough with the greatest depth some 280 m offshore. The comparison of the two seabed configurations reveals a substantial shoreline advance between 2005 and 2011 and much shallower depths onshore of the trough. The

trough and the bar do not show important changes though, and at a depth of some 7.5 m both profiles converge to the nearshore depth of closure. In general, profiles with one dominant bar occur quite frequently at soft cliff beaches. Their behaviour is usually related to general cliff morphology, which in turn is closely connected with its sedimentary composition; sediment migration patterns resulting from cliff erosion are then fully or partly responsible for one-bar nearshore bathymetries.

Rudowski (1965) presented a study on the geological composition of that cliff. Its general morphological characteristics are two seaward looking slopes: a landward-located primary one, subject to weathering due to precipitation and frost, and a secondary one, affected by both weather and wave action. The former is much higher, and the products of its weathering form a seaward-exposed wash slope, separating it from the latter, which is nearshore located and significantly lower. The primary slope is made of layers of sand, red-brown till, sand and gravel mixture, etc. of generally post-glacial origin. The secondary slope is composed of older deposits at its base (Miocene sand and silt, sometimes with remnants of tree trunks) overlain from bottom to top by gravel, sand-gravel mixture, varve clay and gravel with lumps of varved clay. During storms, wave reflection against the cliff toe plays an important role there, and loamy and clayey sediments, making up a large part of the cliff volume, are washed away. Only grains with larger diameters can remain in the surf zone, producing a one-bar system. Again, a study on sediment composition in the bar and trough is recommended to understand what sandy sediments can remain in the nearshore region and contribute to wave energy dissipation. The presence of just one bar may signify that under harsher hydrodynamic conditions, related to the expected climate change effects, the rate of cliff erosion may be significantly intensified with potentially adverse consequences to its hinterland. Thus, the information on sedimentary characteristics of nearshore bathymetry should be ascertained for future coastal zone management purposes as decision support.

The resemblance between the two surveys with respect to key morphologic features (locations and magnitudes of the bar and the trough) justified the computation of the empirical equilibrium profile for the seabed configuration of 2005 only. It consists of three modes of variability, which contain 96.1% of total survey variance and reproduce the actual seabed configuration with high accuracy. The most important characteristic of the actual seabed configuration is the inflection point some 330 m offshore at a depth of about 3.5 m. The shape of the empirical equilibrium profile onshore of that depth is somewhat similar to that of the Dean curve. Therefore, it can be assumed that the saturated wave breaking regime can develop there. The least-square fit of the Dean function to the empirical equilibrium profile yielded $A = 0.085 \text{ m}^{1/3}$, and the saturated rate of wave energy dissipation was evaluated at $E_r = 96.5 \text{ W/m}^2$, using Eq. (4). Offshore of that inflection point, seabed changes are not prominent and converge at about 7.5 m. Wave energy dissipation beyond the nearshore closure depth is negligible, so it can be assumed it is initiated at that depth (7.5 m) and becomes saturated at 3.5 m. In all, the concept of saturated wave energy dissipation in the form

of the beach equilibrium profile is fully applicable at km 130. On the other hand, the presence of a significant amount of cohesive fine sediments within the cliff body implies that, when eroded, these sediment fractions are transported far offshore and do not contribute to coastal stability anymore.

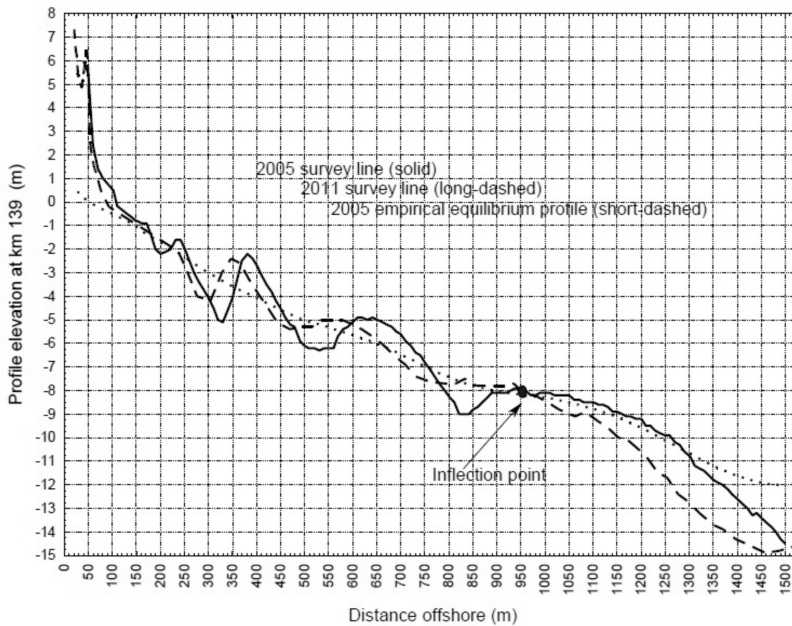


Fig. 5. Empirical equilibrium profile at km 139, after (Różyński and Szmytkiewicz 2018)

The next profile analyzed in detail is situated at Ostrowo (km 139), west of Jastrzębia Góra and east of Karwia. Both surveys are plotted in Fig. 5. We can see that general morphological characteristics of the two surveys are the same, although in 2011 the bars and the shoreline moved onshore, so the beach underwent some erosion. Fig. 5 also shows the results of analysis. From the geological point of view, km 139 belongs to the longest dune strip along the Polish coast (Rosa 1963), running from the west edge of the cliff at Jastrzębia Góra to the town of Rowy. The dune strip is chiefly formed by westerly winds (Zawadzka-Kahlau 2008). Near Ostrowo, it has the lowest height and rests on previously deposited peats, gyttias and hummus and sands of marine and eolic origin (Zawadzka-Kahlau 2008). Therefore, these low dunes can face a direct wave attack during the most severe storms when nearshore sandy sediments are depleted and organic soils become exposed to direct impact of hydrodynamic forces. Insufficient sand supply may then lead to catastrophic inundations of the low-lying hinterland. Such past events and their aftermaths were identified (Zawadzka-Kahlau 2008). Therefore, it must always be remembered that the most extreme events can act as tipping points at km 139, being capable of producing drastic

adverse changes in the functioning of the hinterland once it becomes inundated for a longer period. Without human intervention, such consequences may be difficult or impossible to reverse.

However, despite recently observed erosive tendencies of the coast at km 139 (Zawadzka-Kahlau 2008), the recorded bathymetries revealed fairly ample sediment availability and the resulting notable potential for wave energy dissipation in the submerged beach: 5 nearshore bars were discerned in 2005, starting from the small innermost one, whose tiny crest is located at a depth of 1 m. The crests of the remaining, significantly larger 4 bars are located at 1.5, 2.1, 5 and 8 m. The empirical equilibrium profile consists of two modes of variability that contain only 80.2% of the variance of the profile configuration of 2005. However, except for the offshore region of the outermost bar, absolute departures from the original seabed configuration are tolerably small, so the empirical equilibrium profile is acceptable for multiple bars of moderate magnitude. Interestingly, the inflection point, similar to that found at km 130, can be identified at a depth of 8 m. Moreover, its offshore distance is also the same as the offshore distance to the outermost bar, so they are both co-located. The remote location of the inflection point suggests that the entire surf zone morphology is close to the Dean-type regime of saturated wave breaking. The least-square fit of the Dean parameter to the empirical equilibrium profile yielded $A = 0.089$ and $E_r = 103.4 \text{ W/m}^2$, and this value closely resembles the saturated dissipation of wave energy at km 130 (96.5 W/m^2). Interestingly, the region of the outermost bar underwent the smallest seabed change, so it provided basis for the determination of the depth of (nearshore) closure there. However, offshore of the rather flat and long crest of that bar, the two surveys diverged significantly on the offshore slope of the outermost bar at depths visibly greater than 8 m. This phenomenon was also found in other profiles and was discussed in detail in Różyński and Szmytkiewicz (2018).

The next profile is situated at km 149, just east of the mouth of the river Piaśnica, see Fig. 6. As at km 139, the river mouth region currently shows erosive tendencies (Szymczak and Zabłocka 2018), and the exposure of the adjacent dune strip to more intensive wave action may increase the risk of its breaching/overtopping and ultimately lead to catastrophic flooding of the hinterland, with its precious environmental reservations. However, the inundation risk appears to be lower than at km 139, which definitely is a hot spot. Interestingly, storm surges alone are not very dangerous, as they can only produce significant upstream backwatering in the Piaśnica river along a short stretch from the mouth to a weir just downstream of Lake Żarnowieckie (Szymczak and Zabłocka 2018).

In 2005, the nearshore bathymetry exhibited 3 shallow nearshore bars with crests at 0.5, 2 and 3.8 m. The empirical equilibrium profile had 4 modes of variability and matched very closely the 2005 survey line, capturing 98.9% of its variability. There was also an inflection point at 4 m depth, just offshore of the 3rd bar (crest at 3.8 m). The fitted Dean parameter up to the inflection point was estimated at $A = 0.086$, and the related $E_r = 98.2 \text{ W/m}^2$. In 2011, the two innermost bars merged into one

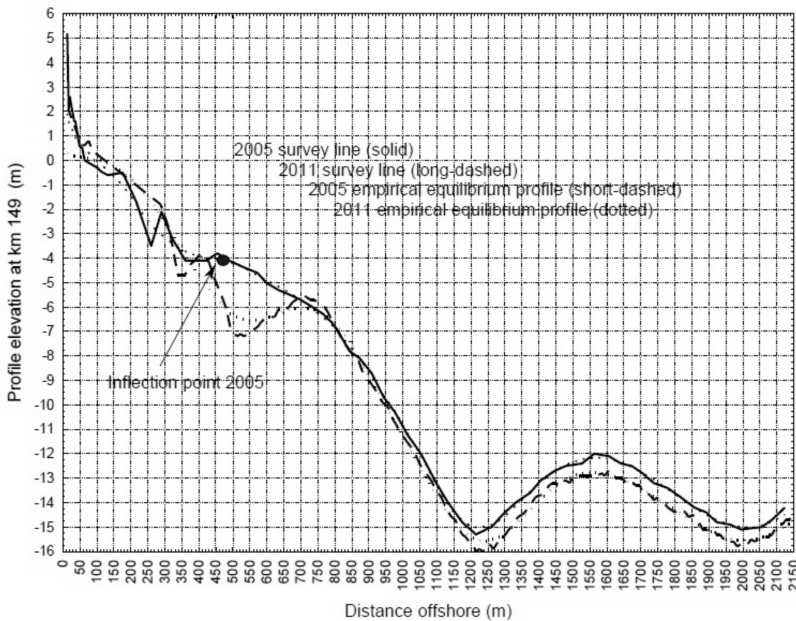


Fig. 6. Empirical equilibrium profile at km 149, after (Różyński and Szmytkiewicz 2018)

quasi-bar structure. The smaller bar remained close to the location of bar 3 from 2005, with its crest at 3.8 m depth, located slightly onshore of the inflection point of the empirical equilibrium profile from 2005. The major difference between the surveys of 2005 and 2011 is a large trough found in the 2011 seabed morphology, with a maximum depth of about 7.3 m, located about 450 m offshore. Further offshore, the seabed of 2011 exhibits a large outermost bar with the crest located 650 m offshore at a depth of 5.7 m. The attempted empirical equilibrium profile retained 98.6% of total seabed variance, but lost monotonicity in the vicinity of the large trough. Thus, the profile at km 149 in 2011 exhibits two types of behaviour: one with the inflection point that delimits the zone of saturated wave breaking and a second, similar to km 125, where a large bar produces two sub-zones of wave breaking regimes. Consequently, this profile line shows mixed behaviour: at times it generates conditions of saturated wave breaking and wave energy dissipation, whereas at other times it forms two separate zones of wave breaking and energy release. Interestingly, both profiles converge just offshore of the crest of the large bar located some 750 m offshore at a depth of about 7 m. This spot defines the (local) nearshore closure depth. The profiles remained close until some 1050 m offshore and 14 m depth. Then, they diverged, and the difference between the depths in the two surveys reached 1 m.

The next profile is located at km 156 near Białogóra, see Fig. 7. In 2005, 3 tiny shallow bars were found at seabed depths of 2, 3 and 3.8 m. The associated empirical equilibrium profile has an inflection point in this region, at a depth of about 3 m and

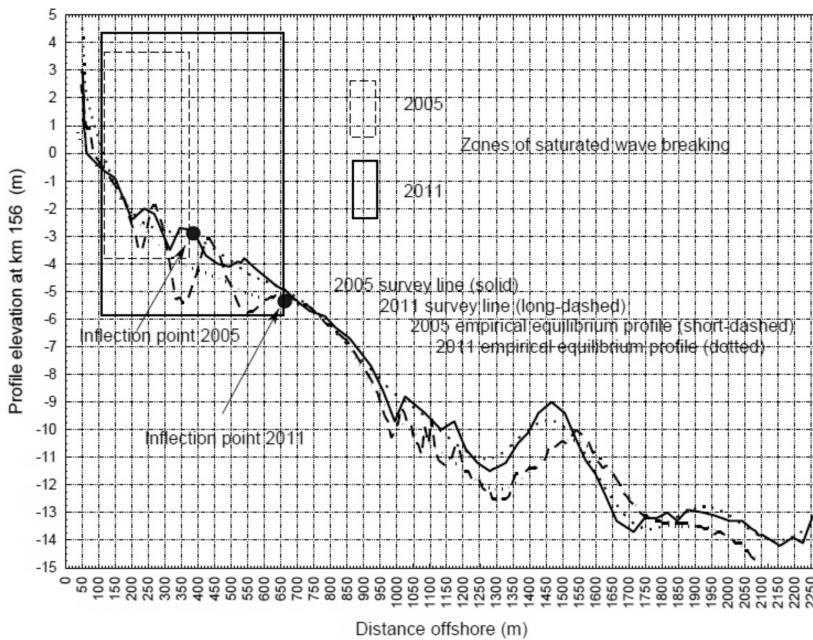


Fig. 7. Empirical equilibrium profile at km 156, after (Różyński and Szymkiewicz 2018)

contains 91.4% of the seabed variance of 2005 in 4 most significant modes of variability. The least-square fitted Dean parameter for this region was $A = 0.069$, which corresponds to $E_r = 70.6 \text{ W/m}^2$. This value points to a lower wave energy dissipation compared with the previously analyzed configurations. The zone of saturated wave breaking for 2005 is rather narrow, extending from the shoreline to the inflection point, see Fig. 7. The seabed in 2011 had some similarities to the profile from 2005, with bar crests at 1.9, 3 and 5.1 m. The main difference was the presence of three deep troughs found in 2011 at 3.5, 5.3 and 5.7 m. As previously, the two profiles converged at about 650 m offshore and opened up again at 900 m with depth discrepancies of over 1 m; the former location corresponds to the nearshore closure depth of 5.5 m. The empirical equilibrium profile for 2011 is plotted as the dotted line in Fig. 7. It contains 93.3% of seabed variance in 4 primary modes of variability. It also has an inflection point at a depth of 5 m, but the zone of saturated wave breaking is wider, see Fig. 7; the corresponding Dean parameter is $A = 0.083$, and $E_r = 93.1 \text{ W/m}^2$. We can see that the zone of saturated wave energy dissipation can persist between measurements separated by as long as 6 years, but energy dissipation itself and the width of saturated energy dissipation can vary. However, it can be tentatively concluded that saturated wave energy dissipation decreases to $70\text{--}100 \text{ W/m}^2$.

An interesting feature at km 156 is a large ‘bar’ located some 1500 m offshore at a depth of 9–10 m. Due to its depth, it cannot be subject to classical wave breaking phenomena. However, the two records show that it can undergo significant migration

over a period of 6 years. It can apparently be interpreted as a continuation of a very large underwater ‘hill’, described in the next paragraph.

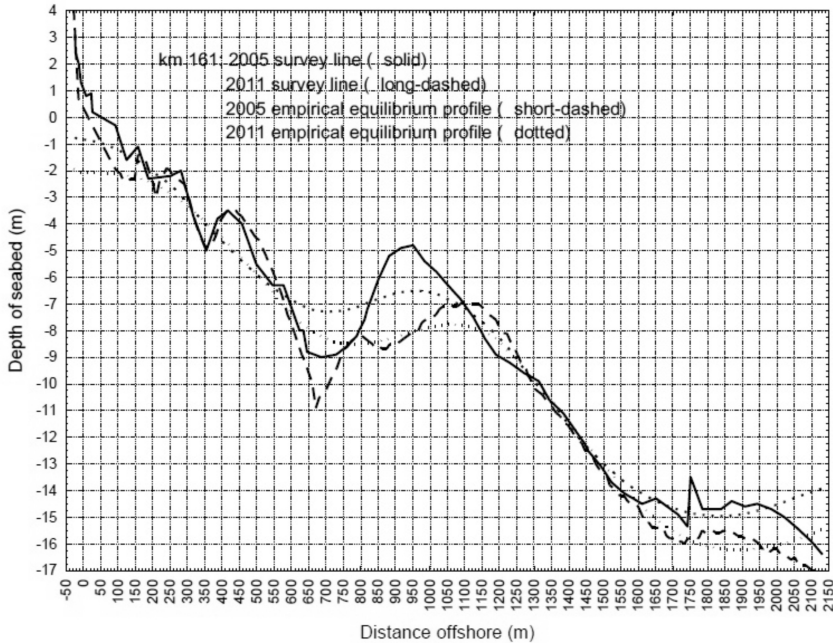


Fig. 8. Empirical equilibrium profile at km 161, after (Różyński and Szymtykiewicz 2018)

Perhaps the most peculiar seabed configuration was discovered at km 161, see Fig. 8. It is characterized by an enormous, remotely located bar (‘hill’), with the crest some 900 m offshore at a depth of only 4.9 m. By contrast, the trough, located some 600 m offshore, had a very large maximum depth of almost 11 m. Closer to the shoreline, three typical smaller bars were discovered with crests at depths of 1, 2 and 3.5 m. The empirical equilibrium profile contained only one mode of variability that captured only 61% of signal variations. The line plotted in Fig. 8 has two modes of variability containing 91.7% of total variability, but it departs significantly from monotonic behaviour. This attempted empirical equilibrium profile points to a situation similar to that found at km 125, which is characterized by the abundance of sediment. However, this abundance is entirely natural, due to locally present sand deposits. The concept of saturated wave breaking is not applicable to this seabed configuration; there are definitely two zones of wave energy dissipation and saturation.

In 2011, the seabed configuration at km 161 was more typical. The very large bar moved offshore, so its crest shifted to 1100 m offshore and sank to a depth of 7 m, whereas the deep trough remained in place, but its depth decreased to 9 m. The other onshore bars remained more or less stable, the only difference being the

shoreline retreat of about 50 m, which was not dangerous, because of the very wide beach. The attempted empirical equilibrium profile for 2011 turned out to be similar to that for 2005, except that it was generally much steeper. This was the result of the offshore translation and sinking of the enormous outermost bar. In general, though, sand abundance produces seabed configurations in which a single zone of saturated wave breaking (and energy dissipation) is not possible. A relatively large time span between the two measurements (6 years) indicates that this situation is stable.

The profile line at km 161 runs through the submerged extension of a large Białogóra dune strip, partly stabilized by forestation in the early 20th century. This region is a NATURA 2000 area PLH220003 and one of its goals is protection of embryonic and developed yellow dunes and grey dunes (Białogóra PLH220003 2015). Using adjacent profiles (not presented in this publication), its western extremity was identified between km 161 and 162; at km 162 the profile line of 2005 displayed three bar crests, with the tiny offshore-most one located just 370 m offshore and having a depth of only 4.2 m. In contrast, the line at km 160 revealed an even greater 'hill' with two crests, 720 and 830 m offshore at a depth of about 5 m. Further east, the profile lines pointed to the eastern extent of that very large bed form at least up to km 154, although the offshore-most bars there are located further offshore and have greater depths. In all, those records indicated a very large local abundance of sand, producing isolated sub-zones of wave energy dissipation, similar to the one identified at km 125. The major difference between them is the purely natural origin of the Białogóra dunes site at km 161 and the entirely anthropogenic origin of the large sand deposit at km 125.

4. Conclusions

In general, the identified wave energy dissipation patterns are highly varied, even though most of the profiles are located on one large morphological unit (the dune barrier from the west end of the cliff at Jastrzębia Góra to the harbour at Rowy). For beaches with very large bars, whether natural (e.g. km 161) or under significant anthropogenic intervention (e.g. km 125), the concept of the equilibrium profile is not valid. In such instances, the surf zone consists of sub-zones where energy dissipation occurs; they are located at offshore bar slopes that culminate at the crest. In troughs, often very deep, energy dissipation does not take place, and broken waves can reform. From the scientific point of view, natural sediment-rich systems are very interesting because the recording of the parameters of reformed waves inside the troughs can provide vital insights into wave transformation and energy dissipation over very large bars during the most severe storms. In the case of less severe events, when the waves mostly refract and diffract without breaking, remote sensing radar campaigns might be advisable for better understanding of these processes. The data collected by radars could then be used in the assessment of the alongshore non-homogeneity of wave energy supply to the shoreline. On the other hand, the study results show that

sediment-rich systems that usually develop isolated sub-zones of energy dissipation between very large bars, serving as sediment buffers, are not usually prone to erosion.

Some profiles, e.g. at km 149, exhibit mixed behaviour. At times, saturated wave breaking regimes can develop, and at other times isolated sub-zones of wave energy dissipation can be detected. It is probably related to the time scales of sediment transport and requires further joint investigations of hydro-, litho- and morphodynamic processes (wave climate, sediment concentration and granulometric distributions in the water column, volumetric changes of beach sediment, etc.).

Most of the profiles exhibited zones of saturated wave breaking and energy dissipation, which can be identified when the empirical equilibrium profile is similar to the shape of the Dean function. Some assessment of energy dissipation intensity can then be given by Eq. (2), or Eq. (4), when the Dean coefficient is evaluated. Usually, such zones start at the shoreline and extend up to the inflection point; the evaluated maximum dissipation rates are about 100 W/m^2 . The length of a segment where the saturated wave breaking regime and energy dissipation can develop and the associated dissipation intensity, are valuable pieces of information that can be used in beach-fill design studies and procedures. The length of saturated wave breaking can be evaluated from the location of the inflection point in the empirical equilibrium profile.

The equilibrium conditions were reproduced from empirical measurements in areas where bars are not very large. Such systems can exhibit erosive tendencies, particularly under changing climatic conditions. This situation is recently observed e.g. at km 139 (Ostrowo), where sand deposits are bounded by deeper strata of organic soils (peat, gyttias, etc.). Therefore, in order to retain sufficient volume of sand in the nearshore region of such areas, intensive beach-fill operations can be carried out, which are routinely designed on the basis of the equilibrium profile theory. One should bear in mind, however, that when sand deposits are confined by clayey or organic soils, additional measures are often needed to achieve the desired beach safety. For example, the dunes at Ostrowo were reinforced by geo-textiles and gabion revetment in 2015 to prevent their overtopping and breaching and to reduce the risk of inundation of valuable nature reserves (Karwia peat bogs). A more general conclusion related to this observation is that, in addition to instantaneous nearshore seabed configuration, it is equally important to know the local geological structure underneath the top stratum of marine sand. Systems with a thin top sand layer can be prone to dramatic regime change in their functioning (tipping point) because depletion of sediment layer during a sufficiently long extreme event can result in uncovering of organic layers. This, in turn, would immediately trigger a radical change in sediment budget, leading to breaching of the dune barrier and dramatic consequences for the hinterland.

The seabed configuration near a soft cliff at km 130 developed a steeper profile with only one bar. This basically results from the washing out and irreversible loss of fine sediment grains from cliffs during storms, intensified by wave reflection from the foot of the cliff massif. Finer grains are transported offshore, and the remaining, coarser sediment can resist wave action and remains in place, producing a seabed

where practically only one bar is present. The equilibrium zone is narrow, but the empirical equilibrium profile is usually monotonic. Also, its departures from the measured seabed configurations are usually small, so empirical equilibrium profiles can be used for the assessment of wave energy dissipation. The saturation of dissipation processes is possible in the narrow sub-zone where the empirical equilibrium profile resembles the Dean function. In general, the presence of one bar reflects general erosive tendencies of soft cliffs on open sea coasts, where wave energy fluxes are only mildly reduced over a bar and shoaling seabed and then attack the cliff foot directly, particularly during storms. Cliff erosion is a natural process, and it is usually not dangerous to the hinterland. The only precaution that should be taken is to delimit an investment safety zone on the cliff top; a rule of thumb of the coastal authorities (Maritime Offices) says that this limit should extend three heights of the cliff landwards of its edge. Possible relaxation of this empirical principle is possible only when a detailed geological analysis of the cliff massif (soil types and direction of strata) has been done.

In summary, this study demonstrates that the concept of empirical equilibrium profile can be applied to the majority of sedimentary coastal systems. Sediment-abundant systems are a major exception, but they usually do not erode and do not need beach fills. Beach-fill operations, however, are usually designed using the equilibrium theory, so the methodology presented here can find numerous applications for such purposes.

Acknowledgements

The research presented in this paper was financed and conducted under the H2020 project HYDRALAB+, contract number 654110 – HYDRALAB-PLUS – H2020-INFRAIA-2014-2015 and mission-related activities of IBW PAN, financed by the Polish Academy of Sciences.

References

- Białogóra PLH220003 (2015) Białogóra PLH220003 – *dokumentacja planu zadań ochronnych (PZO)*, (Białogóra PLH220003 Documentation on conservation management plan) 1-68, <http://pzo.gdos.gov.pl/dokumenty/pzo/item/1742-plan-zadan-ochronnych-obszaru-natura-2000-bialogora-plh220003.html>, access 24th May 2018.
- Bodge K. (1992) Representing Equilibrium Beach Profiles with an Exponential Expression, *Journal of Coastal Research*, **8** (1), 47–55.
- Bruun P. (1954) Coastal Erosion and Development of Beach Profiles, *Technical Memorandum No. 44*, Washington (Beach Erosion Board).
- CEM (2000) *Coastal Engineering Manual*, Part III-3, US Army Corps of Engineers.
- CEM (2000a) *Coastal Engineering Manual*, US Army Corps of Engineers.
- Dean R. G. (1976) Beach Erosion: Causes, Processes and Remedial Measures, s CRC Critical Reviews in Environmental Control, **6** (3), 259–296.
- Dean R. G. (1987) Coastal Sediment Processes: Toward Engineering Solutions, *Proc. Coastal Sediments '87 Conf.*, American Society of Civil Engineers, New Orleans, LA, 1, 1–24.

- Holman R. A., Lalejini D. M., Edwards K., Veeramony J. (2014) A parametric model for barred equilibrium beach profiles, *Coastal Engineering*, **90**, 85–94.
- Inman D. L., Elwany M. H. S., Jenkins S. A. (1993) Shorerise and Bar-berm Profiles on Ocean Beaches, *Journal of Geophysical Research*, **98** (C 10), 18181–18199.
- Komar P. D., McDougal W. G. (1994) The Analysis of Exponential Beach Profiles, *Journal of Coastal Research*, **10** (1), 59–69.
- Kriebel D., Kraus N. C., Larson M. (1991) Engineering Methods for Predicting Beach Profile Response, *Proc. Coastal Sediments'91 Conf.*, ASCE, Seattle, 557–571.
- Larson M., Kraus N. C. (1989) SBEACH: numerical model to simulate storm-induced beach change, *Technical Report CERC 89-9*.
- Moore B. D. (1982) *Beach Profile Evolution in Response to Changes in Water Level and Wave Height*, MSc Thesis, University of Delaware, Newark, USA.
- Özkan-Haller H. T., Brundidge S. (2007) Equilibrium beach profile concept for Delaware Beaches, *Journal of Waterway Port Coastal and Ocean Engineering*, **133** (2), 147–160. [http://dx.doi.org/10.1061/\(ASCE\)0733-950X](http://dx.doi.org/10.1061/(ASCE)0733-950X).
- Pruszek Z. (1993) The Analysis of Beach Profile Changes Using Dean's Method and Empirical Orthogonal Functions, *Coastal Engineering*, **19**, 245–261.
- Rosa B. (1963) O rozwoju morfologicznym wybrzeża Polski w świetle dawnych form brzegowych (On morphological development of the Polish coast in light of past beach forms), *Studia Societatis Scientiarum Toruniensis*, **5**.
- Różyński G., Larson M., Pruszek Z. (2001) Forced and Self-organized Shoreline Response for a Beach in the Southern Baltic Sea Determined through Singular Spectrum Analysis, *Coastal Engineering*, **43**, 41–58.
- Różyński G. (2003) *Coastal Nearshore Morphology in Terms of Large Data Sets*, Gdansk. Institute of Hydroengineering of the Polish Academy of Sciences, 1–170.
- Różyński G., Lin J. G. (2015) Data-Driven and Theoretical Beach Equilibrium Profiles: Implications and Consequences, *Journal of Waterway, Port, Coastal, and Ocean Engineering*, **141** (5). 04015002, Permalink: [http://dx.doi.org/10.1061/\(ASCE\)WW.1943-5460.0000304](http://dx.doi.org/10.1061/(ASCE)WW.1943-5460.0000304).
- Różyński G., Szymtkiewicz P. (2018) Some characteristic wave energy dissipation patterns along the Polish coast, *Oceanologia*, <https://doi.org/10.1061/j.oceano.2018.04.001>.
- Rudowski S. (1965) Geology of the Kępa Swarzewska Cliff, *Annales de la Societe Geologique de Pologne*, **XXXV** (2), 301–318.
- Szymtkiewicz M., Zeidler R. B., Różyński G., Skaja M. (1998) Modeling Large-scale Dynamics of Hel Peninsula, PL, *Proc. 26th ICCE Conference*, ASCE, 2837–2850.
- Szymczak E., Zabłocka B. (2018) Wpływ Zmian Poziomu Morza i Procesów Fluwialnych na Położenie Ujściowego Odcinka Piaśnicy i Litodynamikę Osadów Korytowych (Impact of sea level changes and fluvial processes on the location of the Piaśnica River mouth and the lithodynamics of bed sediments), *Prace Geograficzne*, **152**, 119–132, doi: 10.4467/20833113PG.17.034.8257 Instytut Geografii i Gospodarki Przestrzennej UJ Wydawnictwo Uniwersytetu Jagiellońskiego.
- Zawadzka-Kahlau E. (2008) Morfologiczne efekty oddziaływania czynników hydrometeorologicznych na Mierzei Karwieńskiej (Morphological effects of hydro-meteorological processes at Karwia Spit), *Landform Analysis*, **8**, 88–93.